Australasian Physical & Engineering Sciences in Medicine (2019) 42:627–638
https://doi.org/10.1007/s13246-019-00742-9

TECHNICAL PAPER

Feature extraction using traditional image processing and convolutional neural network methods to classify white blood cells: a study

Roopa B. Hegde[1,2] · Keerthana Prasad[1] · Harishchandra Hebbar[1] · Brij Mohan Kumar Singh[3]

Received: 19 March 2018 / Accepted: 25 February 2019 / Published online: 4 March 2019

Abstract

White blood cells play a vital role in monitoring health condition of a person. Change in count and/or appearance of these cells indicate hematological disorders. Manual microscopic evaluation of white blood cells is the gold standard method, but the result depends on skill and experience of the hematologist. In this paper we present a comparative study of feature extraction using two approaches for classification of white blood cells. In the first approach, features were extracted using traditional image processing method and in the second approach we employed AlexNet which is a pre-trained convolutional neural network as feature generator. We used neural network for classification of WBCs. The results demonstrate that, classification result is slightly better for the features extracted using the convolutional neural network approach compared to traditional image processing approach. The average accuracy and sensitivity of 99% was obtained for classification of white blood cells. Hence, any one of these methods can be used for classification of WBCs depending availability of data and required resources.

Keywords Peripheral blood smear analysis · White blood cells · Classification · Deep learning · Decision support system · Computer aided detection

Introduction

Peripheral blood smear (PBS) analysis is a common laboratory procedure to assess health condition of a person. White blood cell (WBC) analysis plays a vital role in diagnosing many diseases such as leukemia, lymphoma, neutrophilia, eosinophilia, infections etc. There are five types of WBCs namely lymphocyte, monocyte, neutrophil, eosinophil and basophil as shown in Fig. 1a–e. They vary in color, shape, size and texture. Abnormality of WBCs can be present in two ways namely count related disorders and morphology based disorders. Complete blood count (CBC) and differential count (DC) are usually considered in the laboratories to diagnose count related disorders. CBC is performed to provide the total WBC count which includes total count of five types WBCs whereas DC is performed to provide the count of each type of WBCs. Also morphological analysis such as shape, color and size of WBCs are carried out to diagnose diseases such as leukemia, lymphoma etc. WBCs vary in size, shape and color in abnormal conditions as shown in Fig. 1f–j. Abnormal WBCs in the figure include myeloblat, lymphoblat and degenerated WBC. These are immature WBCs and presence of these cells in peripheral blood indicate leukemia. Analysis of WBCs is a laborious procedure and it is burden on hematologists. Automation of detection of WBCs would reduce the workload of hematologists. Also, automated classification of WBCs will lead to faster diagnosis and objective results.

Automation of WBC classification has been addressed since last five decades using traditional image processing approach. This approach involves image processing pipeline consisting of segmentation, feature extraction and classification. These are interdependent steps, hence segmentation of required region and selected features greatly affect the classification results. WBC segmentation is one of the most challenging tasks in medical image processing due to its complex biological appearance, inconsistent staining and

✉ Keerthana Prasad
keerthana.prasad@manipal.edu

1 School of Information Sciences, MAHE, Manipal, India

2 Department of ECE, NMAMIT, NITTE, Karkala, India

3 Kasturba Medical College, MAHE, Manipal, India

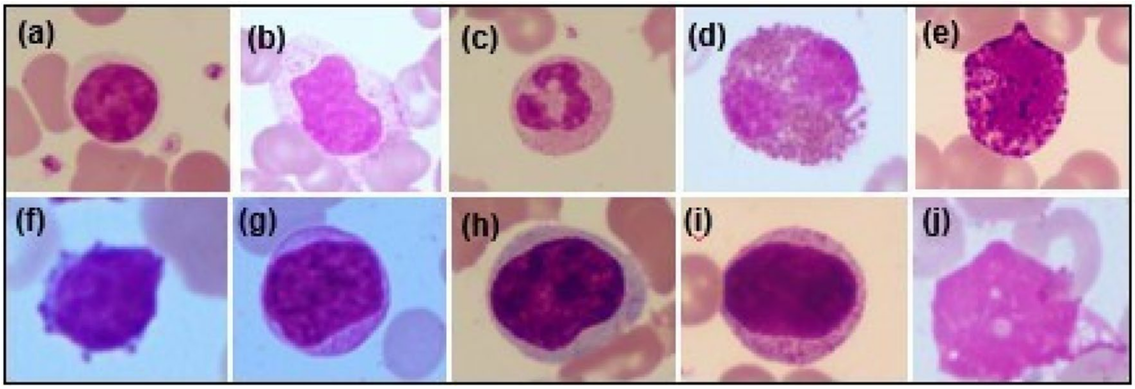

Fig. 1 WBC types; **a** lymphocyte, **b** monocyte, **c** neutrophil, **d** eosinophil, **e** basophil, **f–j** abnormal WBCs

illumination variations in acquired images [1]. Also, quality of images affect the features of medical data [2]. Hence accuracy of classifier may vary depending on the accuracy of segmentation of WBCs and features considered for training the classifier.

Classification of medical images has also been addressed using deep learning approach in the recent years. Convolutional neural network (CNN) is a powerful tool in deep learning method with combination of mathematics and biology [3]. It has gained popularity due to its good performance without having to follow the image processing pipeline. It takes in the raw pixels and processes them in a hierarchical manner and can be used for classification. CNN can be employed for medical image classification in two different ways namely CNN as a classifier and CNN as a feature generator. CNN as a classifier involves efficient tuning of various parameters of different layers of the network which requires large number of training samples. Obtaining large number of expert labeled medical data for training is a difficult task. Also convergence of CNN depends on efficient tuning of the parameters [4]. In CNN as a feature generator approach, features can be extracted from an existing network such as AlexNet, VGGnet, GoogleNet, etc. for a specific dataset which can be employed for small datasets [4]. In this approach, features are extracted from certain layers of the network and later considered for training classifiers. This method of extracting features from CNN provides robust classification [5].

Many researchers tried to automate WBC differential count using traditional image processing approach [1, 6–15]. Neelam et al. [6] compared the results of support vector machine (SVM) and neural network (NN) for classification of WBCs and they reported the accuracy around 97% using NN and 94% using SVM classifier. SVM and NN classifier results were also compared for classification of WBCs by Seyed at al. [13]. Nisha Ramesh et al. [7] proposed an automated method to detect and classify normal WBCs. Segmentation of nucleus was performed considering S component of HSV color model and it was cropped to obtain cytoplasm. They reported classification accuracy of 93.9%. Omid et al. [8] proposed a method for classification of WBCs into its sub-types using SVM classifier. They used color, geometrical, statistical and moment invariant features in their study. They reported the average accuracy of 93%. Hiremath et al. [9] reported classification of WBCs into neutrophil, monocyte and lymphocyte with accuracy in the range of 98–99% They used geometrical features which include area, perimeter, circularity, ratio of major axis length to minor axis length and nucleus to cytoplasm ratio. Sedat et al. [10] compared neural network results with and without using PCA algorithm. They reported the overall accuracy around 95% with PCA and 65% without using PCA for classification of WBCs. Jaroonrut et al. [11] proposed a method for detection and classification of normal WBCs. They used thresholding, morphological operation and ellipse curve fitting for detection of WBCs and Naive Bayes classifier for detection of WBC types. They reported the classifier accuracy around 98%. Naive Bayesian classifier with incremental learning classifier was also used by Mathur et al. [14] for classification of WBCs and they reported overall accuracy around 92%. Subrajeet et al. [15] used NN for segmentation of lymphocyte based on pixel classification. They reported the pixel classification accuracy between 90 and 100% for classification of pixel into nucleus, cytoplasm and background. In order to detect acute myeloid leukemia (AML), Agaian et al. [16] employed a combination of k-means clustering and CIE LAB color space representation for detection of nuclei. The study reported extraction of shape, color and texture features which were used to train a SVM classifier which provided classification accuracy around 98%. Moradi et al. [17] used k-means clustering and SVM for detection and classification of acute lymphoblastic leukemia (ALL). They reported an average classification accuracy around 97%. In order to design a decision support system for diagnosis of ALL using microscopic images, Zeinab et al. [18] used exponential intuitionistic fuzzy divergence and Zack's thresholding methods for detection of nuclei and entire region of WBCs, marker controlled watershed segmentation for separation of overlapped cells and ensemble classifier for detection of leukemic WBCs. The combination of methods used resulted in classification accuracy around 98%. Fatichah [19] employed fuzzy morphology based segmentation method and fuzzy decision tree based classifier for classification of sub-types of leukemia, thereby achieving an average classification accuracy around 84%. Azevedo et al. [20] used a combination of wavelet transform, fuzzy 2-partition entropy, genetic algorithm and morphological operations for segmentation of WBCs considering images of Chronic lymphoblastic leukemia (CLL) cases, thereby reporting an overall Dice score of 0.89.

Many researchers employed CNN as a classifier for classification of medical images [3, 4, 21–25]. Phillip et al. [21] used CaffeNet and VGGNet for classification of abdominal ultrasound images into 11 classes. They reported the accuracy of 90.4% using CaffeNet and 89.7% using VGGNet. Tajbakhsh et al. [4] demonstrated the use of fine-tuning AlexNet considering four distinct medical images from three different imaging modalities. They reported that layer-wise fine-tuning is the practical way to obtain best classification results based on the application and number of training samples. CNN as a feature generator approach was employed by many research groups [3, 22–25]. Atefeh et al. [22] considered extraction of features using AlexNet for tissue classification of coronary artery using random forest and SVM classifiers. They reported the classification accuracy around 96% using random forest classifier and around 94% using SVM. Hyper-spectral image classification was demonstrated by Yushi et al. [3] by extracting features from various convolutional and pooling layers. CNN was employed as feature generator for colonic polyp classification [23] and mass lesion classification of mammogram images using linear SVM classifier [24], with accuracy between 86 and 96%. Mustain et al. [25] extracted features from fully connected layer 2 of the network. SVM classifier was trained using the extracted features to detect gastrointestinal polyp detection in endoscopic images. They reported the detection accuracy of 98.34% and sensitivity of 98.67%.

In the present study, we focused on role of features extracted using traditional image processing approach and CNN as a feature generator approach for classification of WBCs. We extracted shape, color and texture features using traditional image processing approach. Also we used AlexNet which is a pre-trained CNN to extract features. We evaluated the performance of Neural Network (NN) classifier using these features for classification of WBCs and compared the results of the classifier for features extracted using the two approaches. Classification of WBCs has been performed in steps. The first step was to classify WBCs into normal and abnormal and the second step was to classify the normal WBCs into lymphocyte, monocyte, neutrophil, eosinophil and basophil.

Many research groups developed methods for classification of WBCs considering only normal cases [7, 8, 11, 14]. These methods may fail in presence of abnormal WBCs. A few research groups attempted identification of abnormal WBCs but by considering only leukemia cases [16–20]. These methods may fail in presence of any other types of WBCs such as degenerated WBCs. In the proposed method, an attempt was made to classify WBCs considering both normal and abnormal cases so that the method could be practically useful. The abnormal class includes images of leukemia cases, degenerated WBCs, myelocytes and promyelocytes. The main aim of the method is to classify the WBCs into normal and abnormal so that abnormal cases can be sent to pathologists for further evaluation. This helps in faster diagnosis of the abnormal cases.

Materials and methods

This section is divided into three sections namely data collection which is given in "Data collection", feature extraction which is given in "Feature extraction" and classification which is given in "Classification". Our approach in the present study for classification of WBCs is as follows.

- Features were extracted using traditional image processing approach.
- We extracted shape, color and texture features using traditional image processing approach.
- We considered local binary pattern (LBP) representation of grayscale images for extraction of texture features.
- In the 'CNN as feature generator' approach we extracted features from fc6, fc7 and fc8 layers of AlexNet.
- Classification of WBCs was two step process, first step was to classify WBCs into normal and abnormal.
- The second step was to classify normal WBCs into five types namely lymphocytes, monocytes, neutrophils, eosinophils and basophils.
- We used NN classifier to evaluate the performance using the features.
- We compared results of the classifier for the features extracted using the two approaches.

The block diagram representation of our approach is shown in Fig. 2. Input images are color images consisting of a WBC. We considered pre-processing of images as per the requirement of the approaches. In traditional image processing approach, we segmented WBC into nucleus and cytoplasm and features were extracted from

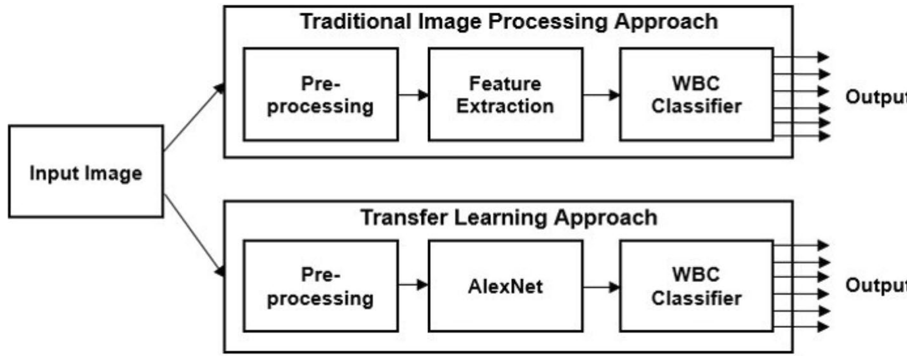

Fig. 2 Block diagram of the present method

both nucleus and cytoplasm. These features were fed to *WBC Classifier* for classification of WBCs.

The *WBC Classifier* is shown in Fig. 3. We used NN classifier in the present study. Classification of WBC is a two step process as shown the figure. In the first step, we classified WBCs into normal and abnormal. In the second step, we classified the normal WBCs into five types as given in the figure.

In the 'CNN as feature generator' approach WBC images were resized as per the requirement of AlexNet. We extracted features from three layers of AlexNet which is a pre-trained CNN. The features extracted from the three layers were separately fed to the *WBC Classifier* for classification of WBCs and results were compared.

Data collection

Images were acquired using OLYMPUS CX51 microscope under 100X magnification with 1600X1200 resolution from hematology laboratory in KMC hospital, Manipal, India. We obtained a total of 280 images from Leishman stained peripheral blood smears consisting of 26 lymphocytes, 28 monocytes, 67 neutrophils, 31 eosinophils, 32 basophils and 136 abnormal WBCs. These images contained RBCs, WBCs and platelets. The groundtruth was obtained from an expert.

Feature extraction

PBS images contain RBCs, platelets, WBCs and staining artifacts. Hence, images were cropped to select WBCs. Small objects such as platelets and staining artifacts were eliminated using image processing techniques such as thresholding, area filter and morphological operations. In the present study we considered handcrafted features and features extracted using deep learning method for classification of WBCs. The details of feature extraction using traditional image processing approach is given in "Traditional image processing approach". The details of feature extraction using deep learning approach is given in "'CNN as a feature generator' approach".

Traditional image processing approach

Features extracted from region of interest (ROI) plays a significant role in classification of WBCs in traditional image processing approach. The block diagram representation of traditional image processing approach is shown in Fig 4. We extracted shape features from nuclei, color features and texture features from nuclei and cytoplasm as shown in the figure.

The shape and size of nuclei of WBCs vary depending on the type of WBC. Hence, we extracted shape features such as area, perimeter, circularity, convexity and solidity from nuclei of WBCs. We also computed nucleus to cell ratio (NC Ratio). The description for the shape features are given in

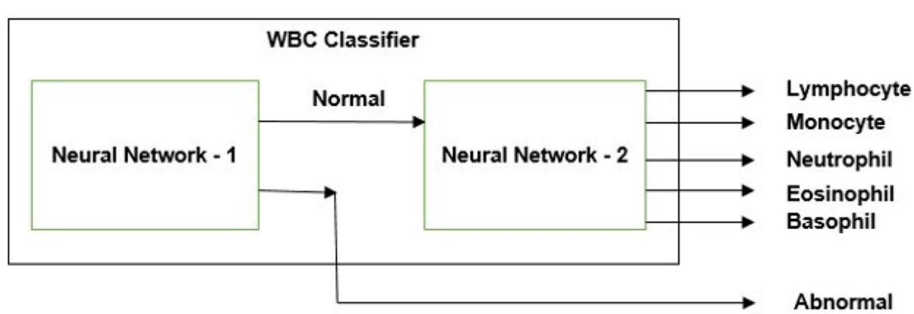

Fig. 3 Block diagram of *WBC Classifier*

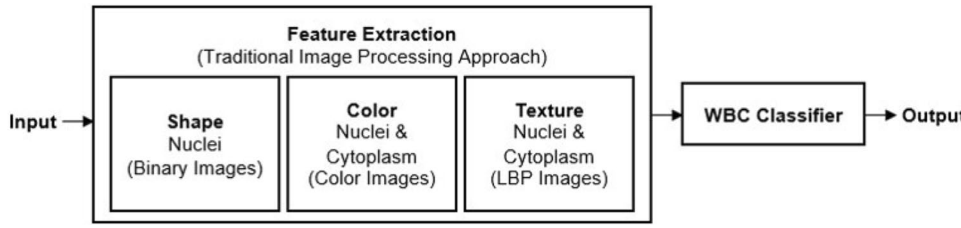

Fig. 4 Block diagram of traditional image processing approach

Table 1 Description of the shape features used in the present study

Feature	Description
Area	Total number of pixels
Perimeter	Path length that surrounds area
Circularity	Perimeter^2/4*pi*area
Convexity	Perimeter of convexhull/perimeter of nucleus
Solidity	Area of nucleus/area of conxhull
NC ratio	Area of nucleus/area of WBC

Table 1. All these shape features were extracted from binary representation of the nuclei.

Color of cytoplasm varies depending on type of WBCs. Also, color variations can be observed in nuclei of WBCs especially in the case of abnormal cells as shown in Fig. 1. Hence, we considered mean and variance of R, G and B components of original color images, H, S and V components of HSV color representation, and L, A and B components of CIE LAB color representation from nuclei and cytoplasm of WBCs as color features in the present study. Depth of color is a distinctive characteristic for classification of WBCs. HSV color space helps in representation of this information. CIE LAB color space helps in managing the illumination variations. CIE LAB and RGB color spaces help in representation of various color shades present in the different types of WBCs.

Texture variation can be observed in both nucleus and cytoplasm of WBCs depending on the type of WBC. We considered LBP representations of grayscale images for extraction of texture features. LBP is a unified approach for statistical and structural texture analysis and is a powerful tool to describe local textures [26]. We used circular LBP of radius 1. The decimal value of resulting LBP given a pixel at (x, y) can be computed as follows.

$$LBP_{(P,R)}(x,y) = \sum_{p=0}^{p-1} s(i_p - i_c)2^p \tag{1}$$

where, P is neighborhood, R is radius, i_c central pixel value, i_p neighboring pixel value. Function s(x) is defined as follows.

$$s(x) = \begin{cases} 1 & \text{if } x \geq 0 \\ 0 & \text{if } x < 0 \end{cases} \tag{2}$$

LBP representations of grayscale images are shown in Fig. 5. In the figure, images in the first row are grayscale representation of original images and images in the second row are LBP images. We extracted texture features such as mean, variance, skewness, kurtosis, spatial gray level dependence matrix (SGLDM) features and Laws texture features from the LBP images.

SGLDM computes 13 features in four directions for angles 0, 45, 90 and 135 degrees. The mean and the range of these features over the four angles are taken as feature set.

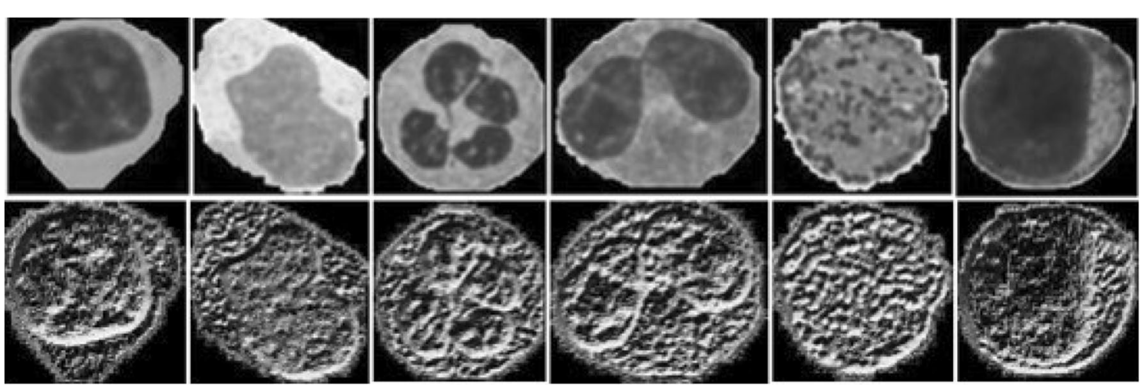

Fig. 5 Feature images; 1st row: Grayscale representation of original images, 2nd row: LBP images

The extracted statistical measures include angular second moment, contrast, correlation, variance, inverse difference moment, sum average, sum variance, sum entropy, difference variance, difference entropy and information measures of correlation. Mathematical relations for these features are given in the Eqs. (3)–(15). The mean and range of these features in all four directions results in 26 texture features.

$$\text{Angular second moment (ASM)} = \sum_i \sum_j p(i,j)^2 \tag{3}$$

$$Contrast = \sum_{n=0}^{Ng-1} n^2 \left[\sum_{i=1}^{N_g} \sum_{j=1}^{N_g} p(i,j) \right] \tag{4}$$

$$Correlation = \frac{\sum_i \sum_j (i,j)p(i,j) - \mu_x \mu_y}{\sigma_x \sigma_y} \tag{5}$$

$$\text{Sum of square (variance)} = \sum_i \sum_j (i-\mu)^2 p(i,j) \tag{6}$$

$$\text{Inverse difference moment} = \sum_i \sum_j \frac{1}{1+(i-j)^2} p(i,j) \tag{7}$$

$$\text{Sum average} = \sum_{i=2}^{2N_g} i p_{x+y}(i) \tag{8}$$

$$\text{Sum variance} = \sum_{i=2}^{2N_g} (i - f_8)^2 p_{x+y}(i) \tag{9}$$

$$\text{Sum entropy} = -\sum_{i=2}^{2N_g} p_{x+y}(i) log[p_{x+y}(i)] \tag{10}$$

$$Entropy = -\sum_i \sum_j p(i,j) log(p(i,j)) \tag{11}$$

$$\text{Difference variance} = \sum_{i=0}^{N_g-1} i^2 p_{x-y}(i) \tag{12}$$

$$\text{Difference entropy} = -\sum_{i=0}^{N_g-1} p_{x-y}(i) log(p_{x-y}(i)) \tag{13}$$

$$\begin{aligned} &\text{Information measures of correlation1} \\ &= \frac{Entropy - HXY1}{max(HX, HY)} \\ &\text{Information measures of correlation2} \\ &= [1 - exp(-2(HXY2 - Entropy))]^{0.5} \end{aligned} \tag{14}$$

$$\begin{aligned} &\text{Maximal correlation coefficient} \\ &= (\text{Second largest eigenvalue of Q})^{0.5} \\ &Q(i,j) = \sum_k \frac{p(i,k)p(j,k)}{p_x(i)p_y(j)} \end{aligned} \tag{15}$$

Laws texture measure is obtained using convolution operation and nonlinear windowing operation on images. The 2D filters for convolution operation are generated from 1D filters namely average gray level (L), edges (E), spots (S) waves (W) and ripples (R). The 1D convolution kernels are as given in the Eqs. (16)–(20). It computes energy of pixels by summing absolute values of convolved output. This produces energy maps whose average values are used as texture measures [27].

$$L = [1\,4\,6\,4\,1] \tag{16}$$

$$E = [1\,2\,0\,2\,1] \tag{17}$$

$$S = [1\,0\,2\,0\,1] \tag{18}$$

$$W = [1\,2\,0\,2\,1] \tag{19}$$

$$R = [1\,4\,6\,4\,1] \tag{20}$$

'CNN as a feature generator' approach

To evaluate CNN as a feature generator for classification of WBCs, we considered extraction of features from various layers of a pre-trained CNN. Also, we compared the performance of the classifier using the features extracted from different layers of the network . The block diagram of CNN as a feature generator approach is shown in Fig. 6. In this case, WBC images were directly given as input to the network. Features were extracted from three layers of the network as shown in the figure. The features extracted from the three layers were used to train the *WBC Classifier* separately as shown in Fig. 6.

We considered AlexNet [28] which is a pre-trained CNN for extraction of features. Hence, all the images were resized to 227x227X3 as per the network requirement. AlexNet is an eight layer network with five convolutional layers (Conv1 - Conv5) and three fully connected layers (fc6, fc7 and fc8) as shown in Fig. 7. Each convolution layer is followed by rectifier linear unit (ReLU) and max pooling operations.

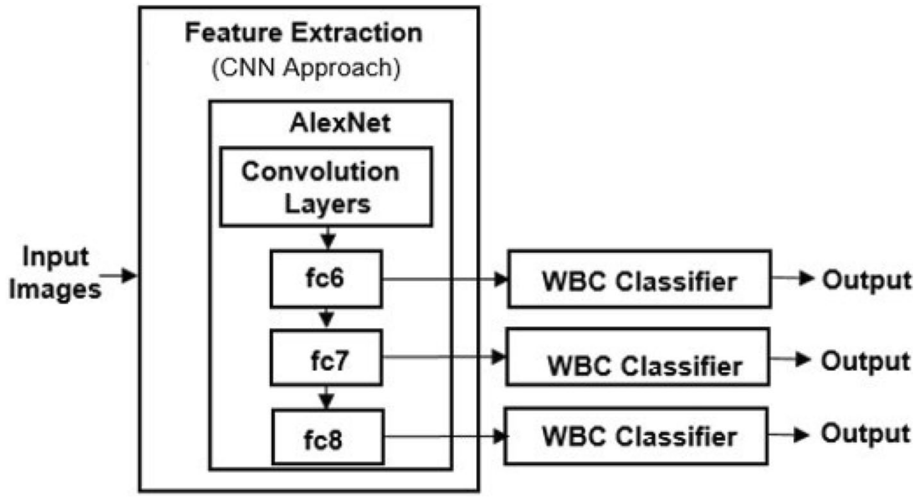

Fig. 6 Feature extraction using 'CNN as a feature generator' approach

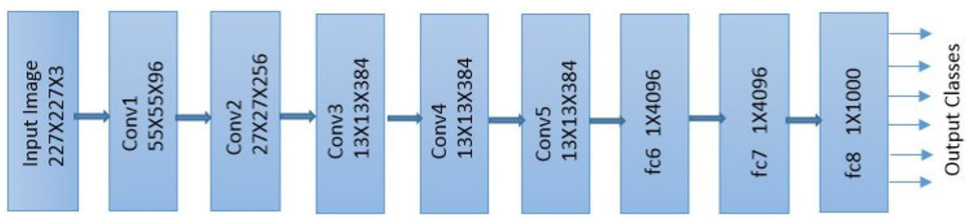

Fig. 7 Architecture of AlexNet

The last fully connected layer gives the output classes using softmax classifier.

Convolution layers extract features from input images using convolution operation. It uses filters to produce features from images. The size of the output of convolution layer depends on number of filters and size of filters. Hence, it reduces the size of the input image. ReLU replaces all negative pixel values of feature map (output of convolution layer) by zero. Pooling layer is used to reduce the dimension of the feature map. Different pooling operations can be used, such as max pooling, average pooling and sum pooling. Max pooling is used in AlexNet. In max pooling, largest element is considered for the defined neighborhood.

The network learns features of the input images in a hierarchical manner. The initial layers learn low-level features and subsequent layers learn high-level features. We extracted features from fc6, fc7 and fc8 layers of the network as shown Fig. 6.

Classification

Features were extracted using traditional image processing approach and 'CNN as a feature generator approach'. To explore the suitability of the features, these features were fed to *WBC Classifier* separately for classification of WBCs. In the present study, classification of WBCs was performed using two steps using the extracted features. The first step was to classify WBCs into normal and abnormal. In the second step, we classified the normal WBCs into five types lymphocytes, monocytes, neutrophils, eosinophils and basophils.

We used NN for classification of WBCs. It is a supervised machine learning method which is inspired by biological nervous system. It consists of input layer, hidden layer and output layer. These layers are linked by weighted connections as shown in Fig. 8, which play a vital role in pattern recognition and classification. In the figure, X_1 to X_n are number of features given to the input layer. Therefore number of nodes in input layer is always equal to number of features given to the network. W_1 to W_n are weights associated with the connections. Number of nodes in hidden layer is application specific. Output from the input layer is fed to the hidden layer and summation and data transformation takes place in this layer. The number of nodes in output layer is equal to the number of classes in specific application. Connections from hidden layer to output layer are weighted connections. These weights are adjusted to match the patterns with labels provided during training.

We extracted a total of 113 features which include shape, color and texture features using traditional image processing approach as given in "Traditional image processing approach". These features were used to train the NN classifier. Also the features extracted from the three layers of AlexNet were used to train the classifier to evaluate the performance. We used hidden layer size of 20 with sigmoid function as activation function. Scaled conjugate gradient back-propagation with cross

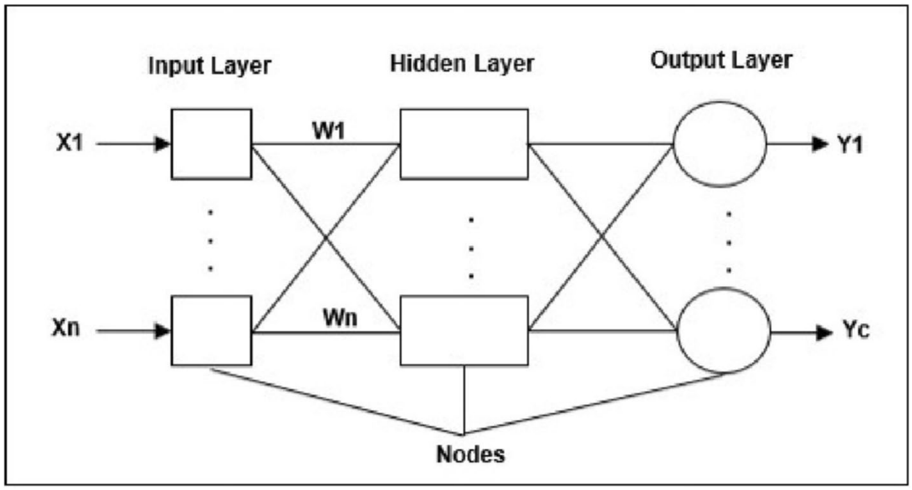

Fig. 8 Simple neural network architecture

Table 2 Confusion matrix for classification of WBCs into normal and abnormal

	Actual normal	Actual abnormal
Predicted normal	183	0
Predicted abnormal	1	136

Table 3 Classifier results for classification of normal WBCs into five types using traditional image processing approach

Performance measure	Value (%)
Average accuracy	98.4
Average sensitivity	98.4
Average specificity	98.1

entropy error function was used during training with random initialization of weights. We used 80% of the data for training and remaining 20% for testing to evaluate the performance of the classifier.

Results

In this section, we provide the results of a comparative study of the two approaches for features extraction. To understand the role of the features, we evaluated the classifier performance separately for the features extracted using the two approaches. Results of the classifier for the features extracted using traditional image processing approach are given in "Classifier results using traditional image processing approach". Performances of the classifier for the features extracted from AlexNet are given in "Classifier results using 'CNN as a feature generator' approach".

Classifier results using traditional image processing approach

We extracted shape, color and texture features using traditional image processing approach. These features were used to train the *WBC Classifier* for classification of WBCs. In this section, the results for classification of WBCs into normal and abnormal, and classification of the normal WBCs into five types are demonstrated.

The results of NN classifier in terms of accuracy, sensitivity and specificity for the features extracted are tabulated in Table 2. It can be observed that, we obtained accuracy of 99.7% for classification of WBCs into normal and abnormal. Also, sensitivity of 100% is obtained for detection of abnormal WBCs as given in the table. This implies that, all the abnormal WBCs are categorized correctly under abnormal class.

We considered classification of the normal WBCs into five types namely lymphocyte, monocyte, neutrophil, eosinophil and basophil as shown in Fig. 3. Performances of the classifier for the features extracted using traditional image processing approach are listed in Table 3. The table shows the average values of the classifier performance. The average accuracy is computed from accuracy obtained for the five classes. The confusion matrix is shown in Fig. 9 which gives classification results of the types of WBCs. In the figure, class 1 represents lymphocyte, class 2 is monocyte, class 3 is neutrophil, class 4 is eosinophil and class 5 is basophil. It can be observed from the figure that, the values of performance measures remain above 93% for detection of all the five types of WBCs. Also, it can be observed from the figure that, accurate detection can be obtained for lymphocytes and basophils using the combination of extracted features and the classifier.

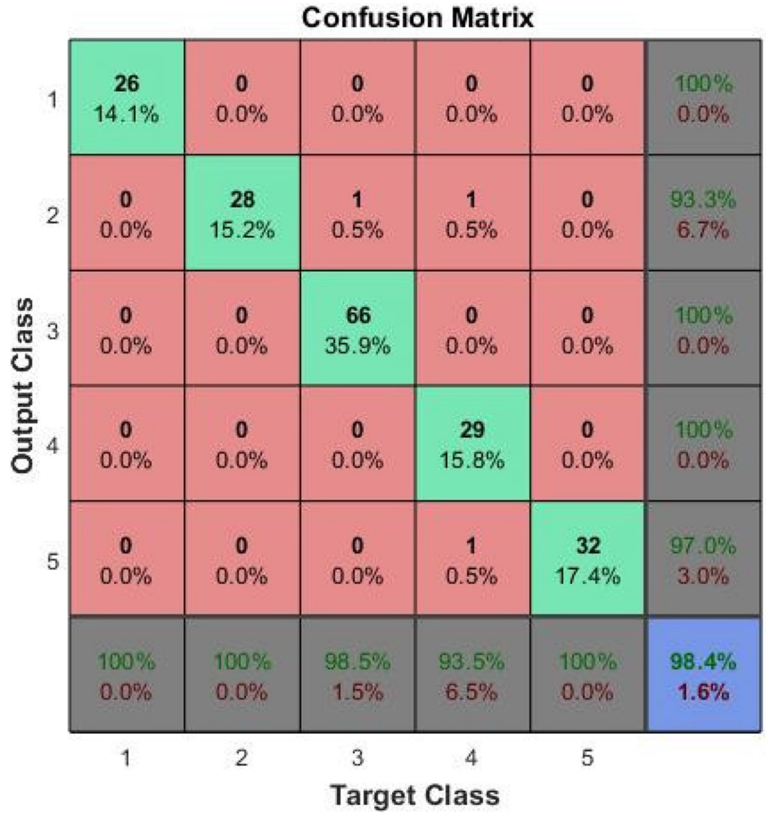

Fig. 9 Confusion matrix for classification of normal WBCs using traditional image processing approach

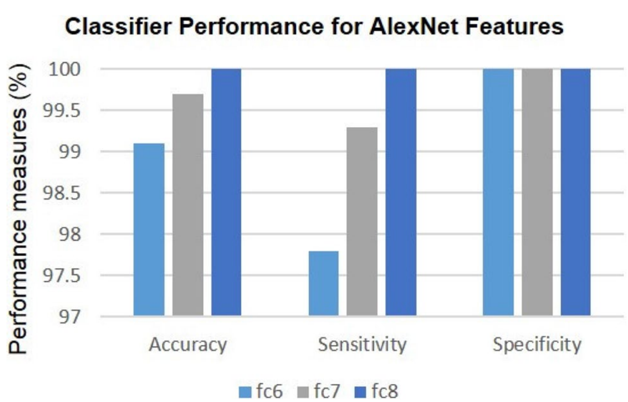

Fig. 10 Classifier results for WBC classification into normal and abnormal using CNN as feature generator

Classifier results using 'CNN as a feature generator' approach

We also considered classification of WBCs into normal and abnormal using the features extracted from the three layers of AlexNet. We extracted features from fc6, fc7 and fc8 layers of AlexNet. Two fully connected layers; fc6 and fc7 layers provide 4096 features each and fc8 layer generates 1000 features. To explore the suitability of the features of the three layers, we evaluated performance of NN classifier by considering these features separately for training the classifier.

Table 4 Performance of NN for features extracted from AlexNet for classification of normal WBCs

Layer	Average accuracy(%)	Average sensitivity (%)	Average specificity (%)
fc6	98.4	98.3	98.5
fc7	98.9	98.6	98.7
fc8	98.9	99.1	99

Performance of the classifier was evaluated by computing accuracy, sensitivity and specificity as in the case of traditional image processing approach. The bar plot for accuracy, sensitivity and specificity for features extracted from all the three layers are shown in Fig. 10. It can be observed from the figure that, accuracy and sensitivity of the classifier is higher for the features extracted from fc8 layer of AlexNet and it is 100% for classification of WBCs into normal and abnormal. Gradual increase in accuracy and sensitivity can be observed from the features of fc6 layer to features of fc8 layer.

The features from fc6, fc7 and fc8 layers of AlexNet were fed to NN classifier for classification of normal WBCs into five types. We evaluated performance of NN classifier by considering these features separately for training the classifier. The average values of the performance measures for the features of the three layers are listed in Table 4. It can be observed from the table that, NN performs equally well for

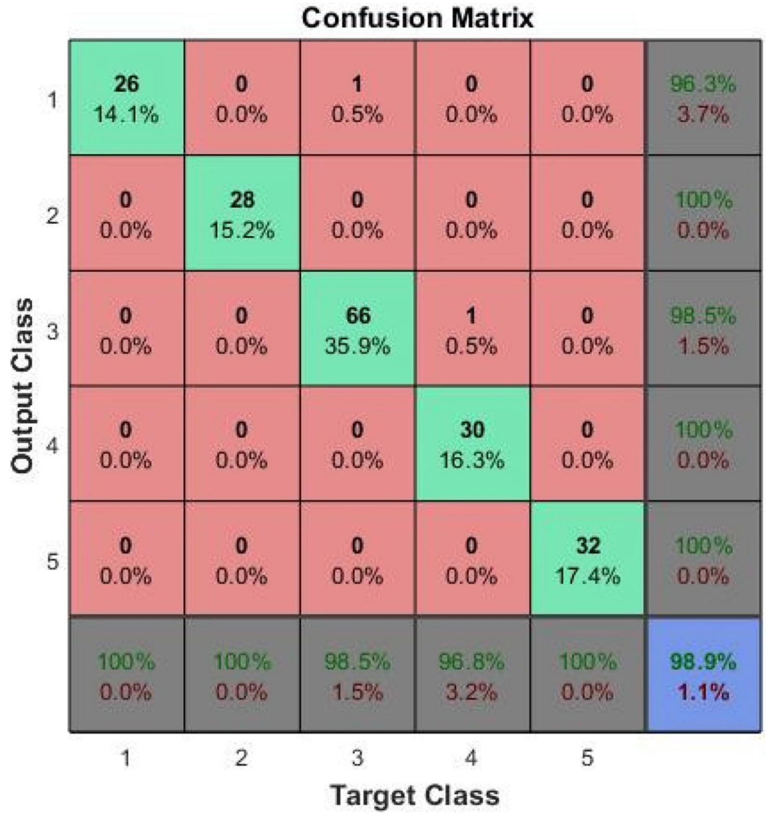

Fig. 11 Confusion matrix for features extracted from fc8 layer of AlexNet for classification of normal WBCs

the features extracted from fc7 and fc8 layers of the network with average accuracy around 99%. The confusion matrix for features extracted from fc8 layer is shown in Fig. 11. It can be observed from the figure that, the values of performance measures remain above 96% for detection of all the five types of WBCs which is higher compared to traditional image processing approach. Also, we obtained 100% accuracy for detection of lymphocytes and basophils as in case of traditional approach. The average detection accuracy is higher using the CNN approach compared to the traditional image processing approach.

Discussion

There are five types of WBCs namely lymphocyte, monocyte, neutrophil, eosinophil and basophil. They vary in shape, size, color and texture as shown in Fig. 1a–e. The change in the appearance of WBCs can also be observed in the case of abnormal conditions. Images shown in Fig. 1f–j are a few abnormal WBC images of our dataset. Variations in color, size and texture can be observed in the depicted WBCs. These variations are the key features to distinguish WBCs. We considered extraction of shape features, color features and texture features under traditional image processing method. We also considered feature extraction from various layers of AlexNet under 'CNN as a feature generator' approach. We trained the NN classifier using the extracted features to classify WBCs into normal and abnormal. Further, the normal WBCs were classified into five types to provide the DC of WBCs.

We obtained the average accuracy of 99.7% and sensitivity of 100% for classification of WBCs into normal and abnormal using handcrafted features. Also we obtained average accuracy of 98.4% for classification of WBCs into five types. Out of five types of WBCs neutrophils and eosinophils consist of lobulated nuclei whereas lymphocytes and monocytes consist of non-lobulated nuclei. The considered shape features mainly help in distinguishing the WBCs into lobulated and non-lobulated nuclei. The color features extracted from cytoplasm help in distinguishing neutrophils and eosinophils. Also, it can be observed from Fig. 1 that, color of nuclei of abnormal WBCs vary significantly. Thus color features extracted from the nuclei contribute in detection of normal and abnormal WBCs. The nuclei and cytoplasm of WBCs show different texture patterns depending on the type of WBCs. Thus the use of LBP representation for texture feature extraction which highlights the local texture features provided the accurate detection of WBCs.

We also used the features extracted from the three layers of AlexNet for classification of WBCs. We obtained 100% accurate result for classification of WBCs into normal and abnormal using the fc8 layer features which is better compared to the accuracy obtained using traditional image processing approach. Also accuracy and sensitivity of 99% was obtained for classification of normal WBCs into five types. This could be due to the well-known fact that, deep networks learn better compared to traditional networks with sufficient number of training images. Also in this approach, WBC images can be directly used and the features are taken care by the network and it is robust to noisy data which is common in microscopic images. In CNN, initial layers learn basic features such as edges, corner, lines etc. which are not sufficient for classification and the succeeding layers derive application specific features. This could be the reason for better accuracy for features of fc8 layers compared to fc6 and fc7 layers.

We obtained 100% accuracy for the detection of lymphocytes and basophils using both the approaches. The reason for accurate detection of these two WBCs is the uniqueness in their appearance. The nucleus of lymphocyte is circular and its cytoplasm is pale blue. Basophils consist of dark blue colored numerous granules which cannot be observed on other type of WBCs. This implies that, the considered features under traditional approach can be used for accurate detection of WBCs. Also AlexNet can be considered as a feature generator for classification of WBCs.

In the present study, we considered classification as two step process. The first step provides the complete count of normal and abnormal WBCs whereas the second step helps in DC thereby providing counting of each type of WBCs. Thus the proposed method can provide the diagnosis based on morphology as well as diagnosis based on DC of WBCs. We observed that, normal and abnormal cells can be detected with 100% sensitivity using the handcrafted features and also using the features of fc8 layer of AlexNet. In an automated system, it is important to detect abnormal WBCs with 100% sensitivity to provide proper diagnosis to individual by sending abnormal cases for expert opinion. The average values of classifier performance obtained for normal and abnormal classification was better compared to the five classes. This is because of overlap of features while considering classification WBCs into five types. Shape and size features of nuclei of neutrophil and eosinophil are almost similar. Though the color and texture of cytoplasm of these two cells show variations, these features may also appear almost similar with illumination variations. Also the features of monocyte and lymphocyte may overlap with change in the illumination source, staining method etc. Hence, features used in classification affects the performance of the classifier. CNN is found to be more useful in this scenario provided the dataset is large enough and computational resources are available.

Classification of WBCs into normal and abnormal leads to faster diagnosis and it also reduces the burden on hematologists/pathologists. Only abnormal cases can be sent for further manual evaluation, hematologists/pathologists need not look into the normal cases provided the sensitivity of detection of abnormal WBCs is 100%.

It can be observed that, both the approaches have comparable accuracy but misclassification is more in case of the traditional approach compared to that of CNN approach. However CNN approach may require more computational resources. From Table 2 it can be observed that, out of 184 normal WBCs one WBC has been misclassified. Considering PBS analysis which uses around 100 views represented by 100 images, misclassification of one WBC would not affect the diagnostic decision making. Hence, traditional image processing would also offer almost equal performance and would be preferable where computational resource is a constraint.

Conclusion

In the present study, we considered traditional image processing approach and CNN as a feature generator approach for feature extraction. Classification of WBCs were performed in two steps. First step was to classify WBCs into normal and abnormal and second one was to classify the normal WBCs into five types namely lymphocyte, monocyte, neutrophil, eosinophil and basophil. We extracted shape, color and texture features using traditional image processing method. We considered LBP representation of grayscale images for texture feature extraction as it highlights the local textures. To explore the suitability of features for classification of WBCs, we also extracted features from various layers of pre-trained network using 'CNN as a feature generator' approach and compared the results. We employed AlexNet, a pre-trained CNN as feature generator. We evaluated the NN classier results using the extracted features. We obtained comparable accuracy using both the approaches. However the performance of the classifier was found to be slightly better for the features of fc8 layer of AlexNet for classification of WBCs. We obtained the accuracy of 99.7% for classification of WBCs into normal and abnormal and average accuracy of 98.9% for classification of normal WBCs into five types. Hence, both traditional image processing approach and 'CNN as a feature generator' approach provide promising results which can be used for classification of WBCs. However training of CNN requires large dataset and high computing resources in comparison with traditional image processing approach.

Compliance with ethical standards

Conflict of interest The authors declare that they have no conflict of interest.

Ethical approval Peripheral blood smear images are obtained from Kasturba Medical College (KMC). This study does not involve human subjects. KMC obtains patient content for using the de-identified archieve data for research purposes.

References

1. Madhloom HT, Kareem SA, Ariffin H, Zaidan AA, Alanazi HO, Zaidan BB (2010) An automated white blood cell nucleus localization and segmentation using image arithmetic and automatic threshold. J Appl Sci 10(11):959–966
2. Takaaki T, Mitsuru I, Kuniharu I, Chiyo Y-K, Katsuhiko K, Haruo I (2013) A new automated assessment method for contrast-detail images by applying support vector machine and its robustness to nonlinear image processing. Austr Phys Eng Sci Med 36(3):313–322
3. Yushi C, Hanlu J, Chunyang L, Xiuping J, Pedram G (2016) Deep feature extraction and classification of hyperspectral images based on convolutional neural networks. IEEE Trans Geosci Remote Sens 54(10):6232–6251
4. Tajbakhsh N, Shin JY, Gurudu SR, Hurst RT, Kendall CB, Gotway MB, Liang J (2016) Convolutional neural networks for medical image analysis: full training or fine tuning? IEEE Trans Med Imaging 35:1299–1312
5. Romany FM (2017) Deep-learning-based automatic computer-aided diagnosis system for diabetic retinopathy. Biomed Eng Lett 17:41–57. https://doi.org/10.1007/s13534-017-0047-y
6. Neelam S, Ramakrishan AG (2003) Automation of differential blood count. In: Proc. IEEE conference on convergent technologies for the AsiaPacific region 2:547–551
7. Nisha R, Bryan D, Mohammed ES, Tolga T (2012) Isolation and two-step classification of normal white blood cells in peripheral blood smears. J Pathol Inf 3:10
8. Omid S, Hossein R, Ardeshir T, Hossein BY (2014) Selection of the best features for leukocytes classification in blood smear microscopic images. In: Proc. SPIE—the International Society for optical engineering 9041:8. https://doi.org/10.1117/12.2043605
9. Hiremath PS, Parashuram B, Sai G (2010) Automated identification and classification of white blood cells (leukocytes) in digital microscopic images. IJCA Spec Issue Recent Trends Image Process Pattern Recogn 37(2):59–63
10. Sedat N, Deniz K, Tuncay E, Murat S, Husnu K, Osman EY (2014) Automatic segmentation, counting, size determination and classification of white blood cells. J Meas 55:58–65
11. Jaroonrut P, Charnchai P (2015) Segmentation of white blood cells and comparison of cell morphology by linear and Naive Bayes classifiers. Biomed Eng Online 14(1):19. https://doi.org/10.1186/s12938-015-0037-1
12. Salim A, Emel O, Cigdem GD (2014) A color and shape based algorithm for segmentation of white blood cells in peripheral blood and bone marrow images. J Int Soc Adv Cytom, Cytom Part A 85A:480–490
13. Rezatofighia SH, Soltanian-Zadeh H (2011) Automatic recognition of five types of white blood cells in peripheral blood. Comput Med Imaging Graph 35:333–343
14. Mathur A, Tripathi AS, Kuse M (2013) Scalable system for classification of white blood cells from Leishman stained blood stain images. J Pathol Inf 4:S15. https://doi.org/10.4103/2153-3539.109883
15. Mohapatra S, Patra D, Kumar S, Satpathy S (2012) Lymphocyte image segmentation using functional link neural architecture for acute leukemia detection. Biomed Eng Lett 2:100–110
16. Agaian S, Madhukar M, Chronopoulos AT (2014) Automated screening system for acute myelogenous leukemia detection in blood microscopic images. IEEE Syst J 8(3):995–1004
17. Amin MM, Kermani S, Talebi A, Oghli MG (2015) Recognition of acute lymphoblastic leukemia cells in microscopic images using kmeans clustering and support vector machine classifier. J Med Signals Sens 5(1):49–58
18. Moshavash Z, Danyali H, Mohammad SH (2018) An Automatic and robust decision support system for accurate acute leukemia diagnosis from blood microscopic images. J Dig Imaging 31:1–16
19. Fatichah C, Tangel ML, Yan F, Betancourt JP, Widyanto MR, Dong F, Hirota K (2015) Fuzzy feature representation for white blood cell differential counting in acute leukemia diagnosis. Int J Control, Autom, Syst 13(3):742–752
20. Thana AAT, Rogrio FP, Ramos BV, Alves NL, do Nascimento MZ (2018) Usingwavelet sub-band and fuzzy 2-partition entropy to segment chroniclymphocytic leukemia images. Appl Soft Comput 64:49–58
21. Phillip MC, Harshawn SM (2017) Transfer learning with convolutional neural networks for classification of abdominal ultrasound images. J Dig Imaging 30:234–243. https://doi.org/10.1007/s10278-016-9929-2
22. Atefeh A, Luc D, Nagib D, Farida C (2017) Deep feature learning for automatic tissue classification of coronary artery using optical coherence tomography. Biomed Opt Express 8(2):1203–1220
23. Eduardo R, Andreas Uhl, Wimmer G, Michael H (2016) Exploring deep learning and transfer learning for colonic poly classification. Comput Math Methods Med 2016:16. https://doi.org/10.1155/2016/6584725
24. Arevalo J, Gonzalez F, Ramos PR, Oliveira J, Lopez MG (2015) Convolutional neural networks for mammography mass lesion classification. In: Proceedings of IEEE 37th Annual International Conference on EMBC, pp. 797–800. https://doi.org/10.1109/EMBC.2015.7318482
25. Mustain B, Sajjad W (2018) Gastrointestinal polyp detection in endoscopic images using an improved feature extraction method. Biomed Eng Lett 8:69. https://doi.org/10.1007/s13534-017-0048-x
26. Di H, Caifeng S, Mohsen A, Yunhong W, Liming C (2011) Local binary patterns and its application to facial image analysis: a survey, IEEE Transactions on systems, man, and cybernetics. Part C Appl Rev 41:765–781
27. Laws KI (1980) Rapid texture identification. In: Proceedings of SPIE 0238, image processing for missile guidance 238: 376–380
28. Alex K, Ilya S, Hinton Geoffrey E (2012) Imagenet classification with deep convolutional neural networks. Proc NIPS 1:10971105

Publisher's Note Springer Nature remains neutral with regard to jurisdictional claims in published maps and institutional affiliations.